Coordination Chemistry Reviews 429 (2021) 213638

Contents lists available at ScienceDirect

Coordination Chemistry Reviews

journal homepage: www.elsevier.com/locate/ccr

Fluorescent probes for biothiols based on metal complex

Wenjuan Liu [a,b], Jie Chen [a,b], Zhaochao Xu [a,*]

[a] CAS Key Laboratory of Separation Science for Analytical Chemistry, Dalian Institute of Chemical Physics, Chinese Academy of Sciences, Dalian 116023, China
[b] University of Chinese Academy of Sciences, Beijing 100049, China

ARTICLE INFO

Article history:
Received 9 September 2020
Received in revised form 30 September 2020
Accepted 30 September 2020
Available online 1 November 2020

Keywords:
Fluorescent probes
Biothiol
Metal complex
Coordination
Lumophore

ABSTRACT

Biothiols are small molecules with important physiological functions. Their detection is mainly achieved by changing the fluorescence emission of fluorophores by the nucleophilic reaction ability of sulfhydryl groups. In recent years, based on the coordination ability of sulfhydryl groups and metals, many more fluorescent probes that recognize biothiols have also been reported. We think this is an appropriate time to review progress in this field. In this paper, we systematically reviewed biothiol fluorescent probes based on metal complexes, including metal complexes as acceptors and fluorescent dyes as reporters; or nucleophilic or reduction reactions as recognition mechanisms, and metal complexes as reporters; or a metal complex acts as both an acceptor and a reporter.

Contents

1. Introduction

Biothiols which refer to mainly three biomolecules cysteine (Cys), homocysteine (Hcy) and glutathione (GSH) are the most abundant low-weight-molecules in cells, and play a critical role in human physiology [1,2]. They have similar structures (Fig. 1a), leading to similar chemical properties, but play different roles in different physiological activities (Fig. 1b). Accurate sensing and tracing of these three substances are of great significance for understanding their physiological functions and analyzing related diseases [1,3–9].

Cys is an important non-essential amino acid, which mainly exists in the form of L-cysteine outside the cell. With the help of the active transport of the cell membrane, L-cysteine would enter cell and then be reduced to Cys. Cys can participate in the synthesis of glutathione and sulfur-containing proteins in organisms [10,11]. Therefore, Cys affects the oxidative stress of cells and participates in the regulation of the body's intestinal function, lipid metabolism and other processes [12]. Hcy has received widespread attention

Abbreviations: LOD, limit of detection; GSH, glutathione; Cys, cystein; Hcy, homocystein; Met, methionine.

* Corresponding author.
E-mail address: zcxu@dicp.ac.cn (Z. Xu).

https://doi.org/10.1016/j.ccr.2020.213638
0010-8545/

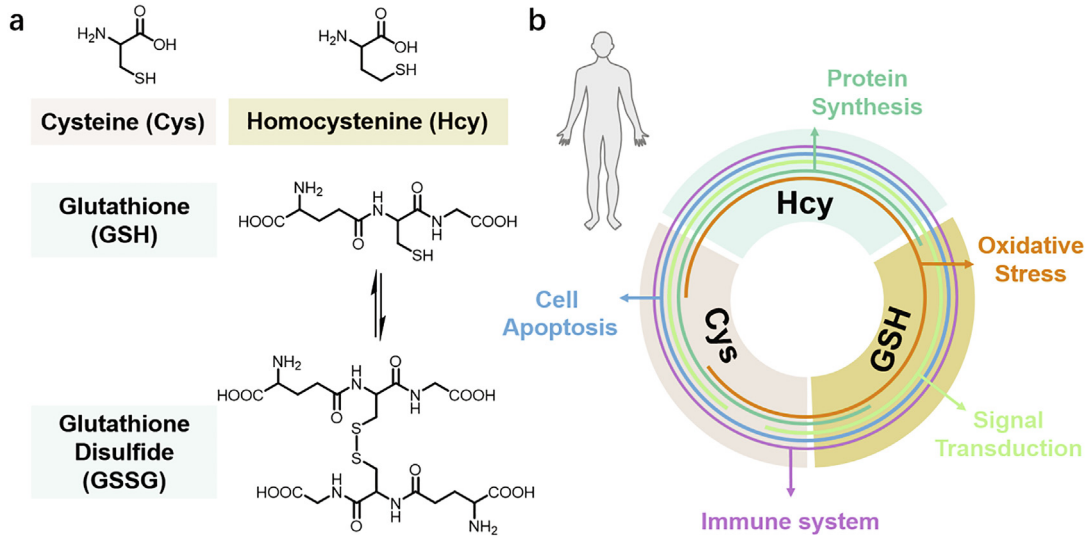

Fig. 1. (a) The structures biothiols; (b) The main physiological functions of biothiols.

due to its close relationship with cardiovascular diseases and aging. Especially as a key indicator of ischemia–reperfusion injury of the heart, cognitive impairment in the elderly and Alzheimer's disease, Hcy has great significance in disease diagnosis and treatment [10,13]. As the most fruitful biothiol in living systems (1–10 mM) [6,7], GSH is the redox center of cells. In fact, due to the mutual transformation between the reduced state (GSH) and the oxidized state (GSSG), the redox balance in the cell can be maintained. Besides, GSH is also directly involved in the production of signal molecule (such as H2S), protein functionalization and other processes, and is a key part of intracellular gene regulation and signal transduction [3,4].

Nowadays, the detection of biothiol in the laboratory are mainly based on electrochemical analysis and high performance liquid chromatography [12,14]. However, those methods only focus on the total content of sample, and always require complex pretreatment in order to obtain a uniform solution, which lead to missed real-time detection of specific subcellular structure. The development of fluorescence probes for thiols has been attracting much more attention in recent years [15–21], due to the advantages of fluorescence including high sensitivity, nondestructivity, *in situ* examination, and intracellular detection. There have been efforts to develop fluorescent probes for detecting biothiols in biological samples, living cells and even living bodies. A typical fluorescent probe contains a reporter (fluorophore) linked to a receptor (the recognition site) and the recognition event is translated into the fluorescence signal. Based on the chemical properties of sulfhydryl groups, most fluorescent probes used the nucleophilic reaction or reduction ability of sulfhydryl groups to identify biothiols. So far, there have been some review papers discussing biothiol fluorescent probes. The fluorescent probes summarized in these papers are mainly based on organic fluorescent dyes [12,22–28]. The first review systematically discussed probes based on different reaction types between probes and sulfhydryl groups in 2010 by Yoon *et al.* [25] During this period, biothiol fluorescent probes developed rapidly, so three years later, the Yoon group once again summarized the new probes reported in 2010–2012 [12]. In the same year, Yin *et al.* also reviewed thiol probes constructed based on Michael addition reaction and their applications in thiol detection [26]. Kaur *et al.* reviewed the reported biothiols fluorescent probes in 2018 based on the principle of spectral changes. Recently, a series of on multiple reaction site probes developed to distinguish biothiols were summarized and reviewed by Yang [27] and Yin *et al.* [28], respectively. In this paper, we systematically reviewed biothiol fluorescent probes based on metal complexes, including metal complexes as acceptors and fluorescent dyes as reporters; or nucleophilic or reduction reactions as recognition mechanisms, and metal complexes as reporters; or a metal complex acts as both an acceptor and a reporter. Metal complexes as acceptors rely on the ability of sulfhydryl groups to complex metal ions. Readers can refer to the published review papers for the principles of the fluorescent signal conversion mechanism used after molecular recognition and how to choose to use these mechanisms [29] Fig. 2.

2. Recognition mechanisms

The biothiols have similar structures and contain three functional units, which are the amino acid skeleton R, the S atom of the sulfhydryl group and the H atom of the sulfhydryl group (Fig. 1a and Fig. 3). The three biothiols differ in molecular structure and chemical activity of the amino acid skeleton R so that the chemical activity of the S and H atoms of the sulfhydryl group are different. Ideal molecular recognition needs to be able to selectively bind the three parts of R, S and H at the same time. The fluorescent probes reported so far were basically based on the difference in the chemical activity of the sulfhydryl group S or H to achieve the purpose of recognizing biological thiols. It has not been seen that one probe can recognize the three functional units of R, S and H simultaneously (Fig. 3a). The recent progress is the introduction of multiple reaction sites in the probe to identify different biothiols, which is mainly based on the difference in the nucleophilic reactivity of the sulfhydryl S. This also inspired the design of future biothiol probes to consider the difference in the coordination ability of sulfhydryl S and the difference in the reduction ability of sulfhydryl H as the recognition mechanism. Applying these three different capabilities to probe design at the same time may bring features beyond imagination.

The chemical activities of the S and H atoms of the sulfhydryl group include nucleophilic reaction ability, coordination ability with metal ions, and reduction ability, respectively. The most common type is to use the nucleophilicity of the S atom to generate cleavage of sulfonamide or sulfonate ester, cyclization with aldehydes and Michael addition with alkenes. Those reactions are usually accompanied by a marked increase in fluorescence (Fig. 3b). The second type of biothiols probes is based on the high binding affinity of sulfur, and is characterized by the displacement of coordina-

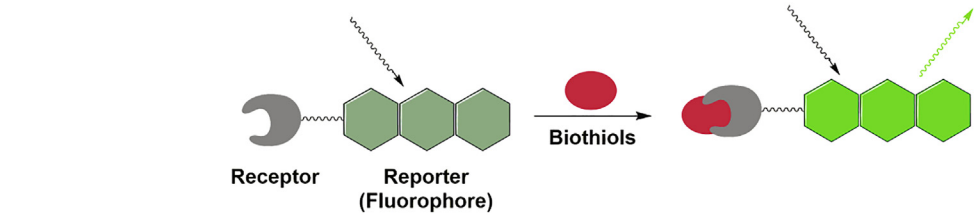

	Recognition Mechanism	Signal Transduction	Fluorophore	Response
previous reviews:	Nucleophilic reaction Reduction	PET ICT FRET Excimer ESIPT	Organic Dyes	Fluorescent Intensity Emission Shift Colorimetric
this review:	**Coordination** **Nucleophilic reaction** **Reduction**	**PET** **FRET**	**Organic Dyes** **Metal Complex**	**Fluorescent Intensity** **Emission Shift** **Colorimetric** **Lifetime**

Fig. 2. Strategies of constructing biothiols detection probes.

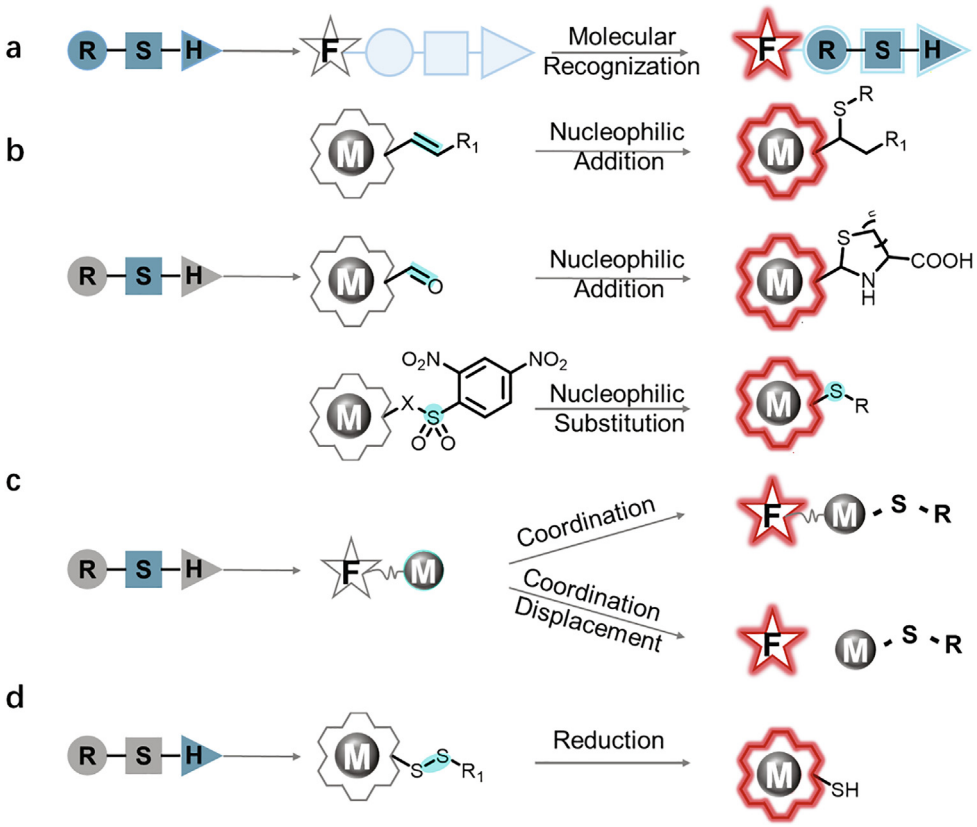

Fig. 3. Mechanisms of biothiols recognized by metal complex probes. a) the molecular recognition of biothiols; b) The nucleophilicity of sulfur was utilized and metal complex worked as a reporter; c) the coordination of sulfur was used and metal complex worked as a receptor; d) the reducibility of the sulfhydryl group was used and metal complex worked as a reporter.

tion structure of chromophore by biothiols. For this type of probe, their fluorescence is usually significantly quenched due to coordination with metal ions (Fig. 3c). The third part is based on the reducibility of the sulfhydryl group. These probes are generally composed of a pair of FRET donor and acceptor connected by a disulfide bond. Once the disulfide bond is reduced by the biothiol, the chromogenic group in the probe is dissociated from the quenching group, and the characteristic absorption and luminescence of the probe are changed to realize the recognition of the thiols (Fig. 3d).

3. Metal complex as a biothiol probe

Metal complexes play an important role in life science. Through changes in ligands, coordination numbers, coordination positions

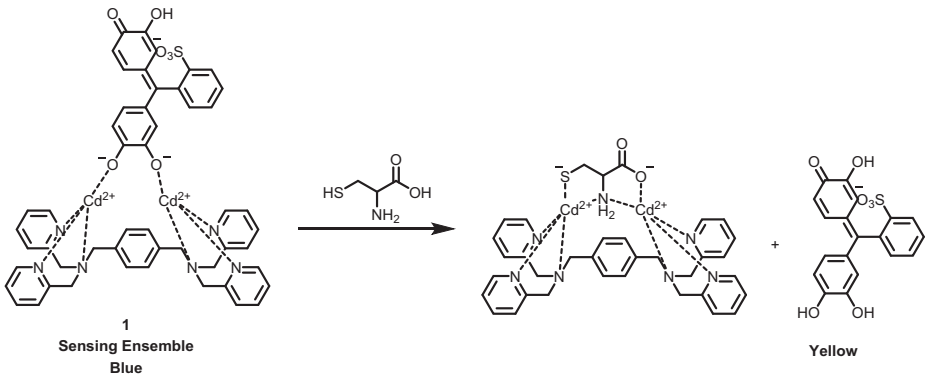

Fig. 4. The sensing mechanism of **1** for Cys.

and coordination capabilities, they mainly act as skeletons in biological macromolecules, regulating redox and signal transduction. For example, the biological functions of zinc ions, copper ions, and iron ions are mainly achieved through coordination and regulation of N, O, and S. Therefore, the recognition of biothiols can be realized by the coordination of the sulfhydryl group to the metal complex. In addition, some lanthanide and transition metal complexes themselves have good luminescence properties. Through reasonable design, molecular probes with long wavelength and large Stokes shift can be obtained [30]. There have already been related reports using those lumophores as reporters for detection of small molecules such biothiols in living systems [31,32].

3.1. Metal complex as a receptor

Most metal complexes can absorb light in the visible region, and heavy metal or transition metal ions have the property of quenching fluorescence. Before and after the coordination of the metal, biothiols will cause a change in the configuration of the metal complex or the dissociation of the chromophore ligand from the complex (Fig. 3c), and the resulting fluorescence enhancement or color change would be used to identify the target thiol.

Kim *et al.* reported the probe **1** for Cys sensing in aqueous buffer (pH 7.0, HEPES, 10 mM) in 2004 [33]. Wherein, the receptor was constructed by the complex $[Cd_2(TPXD)]^{4+}$ formed by cadmium perchlorate and *N, N, N′, N′*-tetra-(2-pyridylmethyl)-p-xylyenedia mine, and the indicator was pyrocatechol violet (Fig. 4). The association constant of **1** binding Cys was reported to be $(1.62 \pm 0.97) \times 10^7\ M^{-1}$, which was one hundred times of that for the binding of the indicator ($(2.77 \pm 0.98) \times 10^5\ M^{-1}$). Then the addition of Cys would displace pyrocatechol violet from the complex. Due to the release of the reporter, a decrease of the absorbance band around 665 nm was observed, associated with the color change from blue to yellow.

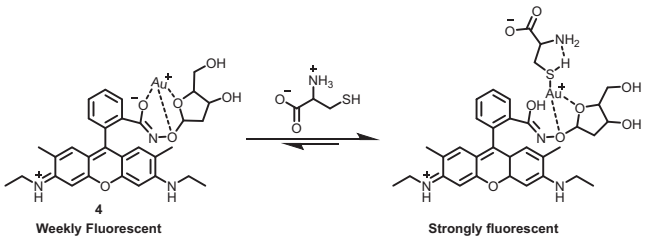

Fig. 5. The sensing mechanism of **4** for Cys.

Fu *et al.* reported an in-situ chemosensing ensemble system **2** for biothiols [34]. After Cu^{2+} was added to the solution of indicator molecular, the fluorescence is quenched, and a 1:1 adduct is formed as the thiol detection system. The coordination displacement of thiol and Cu^{2+} caused the indicator released, following by a significant fluorescence enhancement. The detection system showed high selectivity for Hcy and Cys. Calculations showed that the binding constants for Cys and Hcy at pH 7 were $1.8 \times 10^5\ M^{-1}$ and $1.8 \times 10^5\ M^{-1}$, respectively.

Yang *et al.* reported another fluorescent chemosensor for Cys, which was designed based on the fluorescence inner filter effect (IFE) between **3** and rhodamine B [35]. Upon the addition of Cu^{2+}, the colorless and non-fluorescent spirolactam of **3** changed to the ring-opened zwitterion **3**-Cu^{2+} with pink color and weak fluorescence. Due to the fluorescence internal filtering effect (IFE), the fluorescence signal of co-existing Rhodamine B cannot be detected. Once Cys added, the coordination of Cys with Cu^{2+} disrupted the coordination of **3** with Cu^{2+}, and the IFE was reduced to lead a remarkable increase of rhodamine B fluorescence.

Compared with **3**, the mechanism of fluorescence changes in probe **4** before and after complexing with thiol was much clearer. Yang *et al.* reported probe **4** [36], a turn-on system in which the complex of rhodamine hydroxylamine and Au^+ with 2-deoxyribose acted as the receptor (Fig. 5). The coordination of Au^+ quenched the fluorescence of rhodamine, possibly because the amide group on the benzene ring participated in the complexation. This probe could detect cysteine and homocysteine selectively (water with 1% methanol), and exhibited a significant fluorescence enhancement resulted from the release of amide group on benzene. The detection limit of 4 for Cys was 100 nM through fluorescence titration experiment. The binding stoichiometry was found to be 1:1, and the binding constant was calculated to be $6.65 \times 10^3\ M^{-1}$.

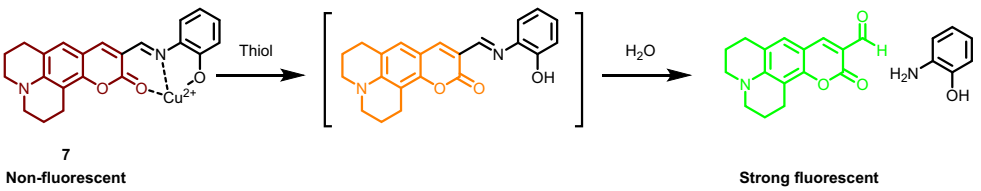

Fig. 6. The sensing mechanism of **7** for Biothiols.

Tsay *et al.* reported a Cys selective sensing ensemble **5** [37] based on the 1:1 complex between *meso*-aryl bodipy and Cu^{2+}, with a good selectivity over glutathione (GSH), homocysteine, *N*-acetylcysteine and methionine. Peng *et al.* reported a probe formed from ion catalyzed reaction [38]. Dibenzo[*a,kl*]xanthen-1-ol (**6**) was oxidized from BINOL by $Cu(NO_3)_2$, and the formed complex with 1 equiv of Cu^{2+} accompanied by a complete quenching of fluorescence. After adding Cys, Hcy or GSH, a new peak at about 482 nm appeared, demonstrating the recognition of biothiols.

Jung *et al.* and Yu *et al.* reported two cases of coumarin-based copper complexes **7** (Fig. 6) and **8** for biothiols detection, and applied to imaging biothiols in living cells [39,40]. The probe **9**

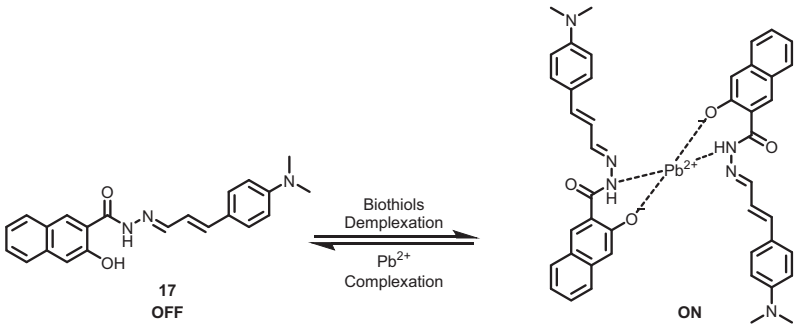

Fig. 7. The sensing mechanism of **17** for Biothiols.

Table 1
Metal Complex as Receptor.

Structure	λ_{abs} (nm)	λ_{em} (nm)	Biothiols	LOD/Binding constant	Responses	Ref.
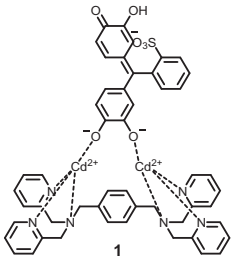 1	444	\	Cys	$(1.62 \pm 0.97) \times 10^7$ M^{-1}	The absorbance at 665 nm decreased and the peak at 444 nm increased upon addition Cys (HEPES 10 mM, pH 7.0).	[28]
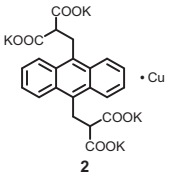 2	\	430	Cys Hcy	1.8×10^5 M^{-1} 3.3×10^5 M^{-1}	The absorption and emission increased after adding Cys/Hcy (HEPES 50 mM, 0.1 M NaCl).	[29]
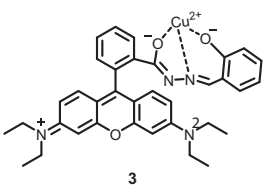 3	558	580	Cys	1.4×10^{-4} M	A decrease of absorption and increase of emission was detected after adding Cys (Ethanol/Tris-HCl, pH 7.1, 2/3, v/v)	[30]
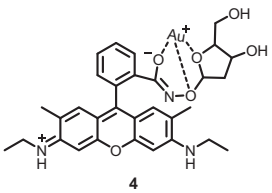 4	500	560	Cys	1×10^{-4} M 6.65×10^3 M^{-1}	A color change from colorless to red of the solution and emission enhancement were observed upon addition Cys (Water, Methanol 1%).	[32]
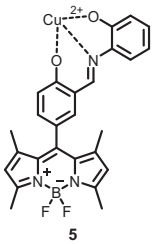 5	499	510	Cys	6×10^{-6} M 3.4×10^4	An enhancement of emission was observed after adding Cys (Methanol/HEPES, pH 6.5, 3/7, v/v)	[32]

(*continued on next page*)

Table 1 (*continued*)

Structure	λ_{abs} (nm)	λ_{em} (nm)	Biothiols	LOD/Binding constant	Responses	Ref.
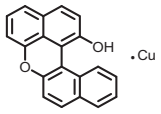 6	305	482	GSH Cys Hcy	1.5×10^3 M^{-1} (Cys)	A new emission peak appeared at ~482 nm upon addition of biothiols (ACN/Water, 1/1, v/v).	[33]
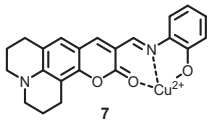 7	479	514	GSH Cys Hcy	1×10^{-8} M (Cys)	A color change from orange to green of the solution and an enhancement of emission at 514 nm were observed (PBS 10 mM, pH 7.4, with 1% DMSO). Intracellular thiols image was obtained.	[34]
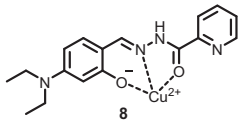 8	428	488	Cys	6.4×10^{-7} M	The absorption peak at 428 nm decreased and blue-shifted to 383 nm, while emission at 488 nm increased (PBS pH 7.4). The living cells image of Cys was obtained.	[35]
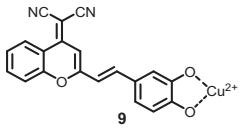 9	570	718	GSH Cys Hcy	6.47×10^{-6} M 4.93×10^{-6} M 4.81×10^{-6} M	An emission enhancement at 718 nm was observed after adding biothiols (Ethanol/PBS, 10 mM, pH 7.4, 3/2, v/v). The probe was applied to image GSH in MCF-7 cells and zebrafish.	[36]
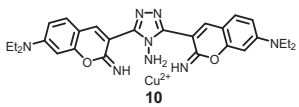 10	410	520	GSH	3.6×10^{-7} M	An emission enhancement at 520 nm was observed after adding GSH (ACN/Water, 1/1, v/v). The imaging of GSH in *E. coli* cells was obtained.	[38]
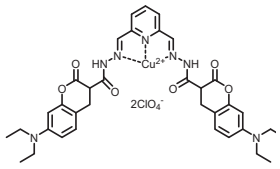 11	440	485	GSH	2×10^{-7} M	An emission enhancement at 485 nm was observed after adding GSH (ACN/HEPES, 3/2, v/v). The imaging of GSH in living cells was obtained.	[39]
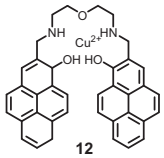 12	355	450	GSH	1.6×10^{-7} M	An emission enhancement at 450 nm was observed after adding GSH (HEPES, 10 mM, pH 7.4, 5% DMSO). Both the two probes were applied for biothiols detection in live cells	[40]
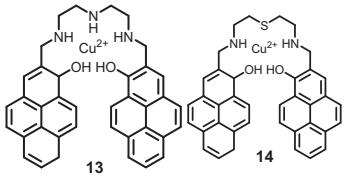 13 14	350	450	GSH Cys Hcy	ND	An emission enhancement at 450 nm was observed after adding biothiols (PBS 100 mM, pH 7.4, 5% DMSO). The probe was applied for biothiols detection in living cells.	[41]
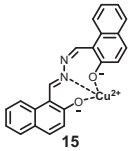 15	411	513	GSH Cys Hcy	8×10^{-7} M 1×10^{-6} M 5×10^{-7} M	The absorption at 475 nm decreased and shifted to 411 nm, while a 47.8-fold enhancement of emission at 513 nm was detected (DMF/HEPES, 20 mM, pH 7.4, 3/7, v/v). The probe was applied for biothiols detection in living cells.	[37]
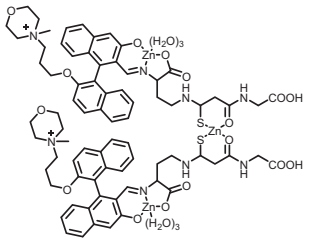 16	430	560	GSH	1.72×10^{-6} M	An emission enhancement at 560 nm was observed after adding GSH (HEPES, pH 7.5).	[42]

Table 1 (*continued*)

Structure	λ_{abs} (nm)	λ_{em} (nm)	Biothiols	LOD/Binding constant	Responses	Ref.
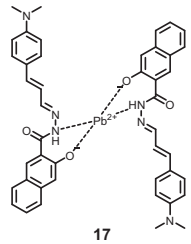 **17**	480	560	GSH Cys Hcy Thiols	5×10^{-7} M	An emission enhancement at 560 nm was observed after adding biothiols (Methanol/HEPES, 1 mM, pH 7.4, 4/1, v/v).	[43]
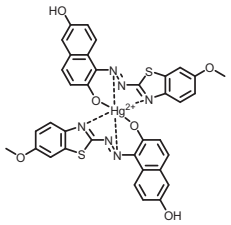 **18**	252	540	Cys	ND	A color change from blue to pink with an enhancement of emission at 540 nm were observed upon adding Cys.	[44]

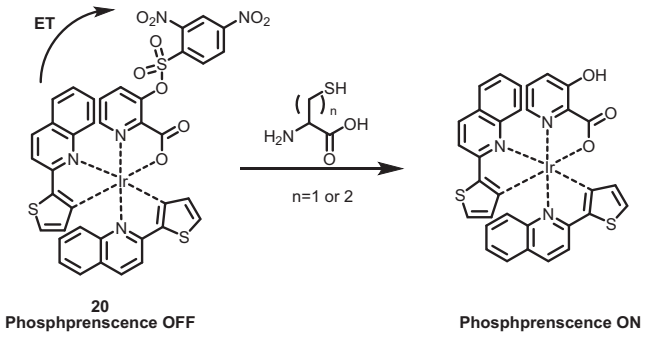

Fig. 8. The sensing mechanism of **20** for Cys and Hcy.

was developed on a similar principle [41]. These probes were all based on the complexation of thiols and copper ions to release fluorophores, resulting in a fluorescence enhancement response.

Probes **10**–**18** were constructed on a similar strategy that a metal complex was conjugated with two identical chromophores. The difference was that there were two chromophores in compounds **10**–**15** [42], which were complexed with the metal in a 1:1 form; while the compounds **16**–**18** each contained one chromophore and complexed with the metal in a 2:1 form. In **10** and **11** [43,44], two coumarins were connected by the ligand of schiff base, and then formed complexes with 1 equiv of Cu^{2+}. The addition of biothiols removed the copper ion from the fluorophores, and the released fluorescence was observed. Those two probes had been successfully applied in biothiol imaging in living cells. Similarly, *Yoon et al.* reported three probes, **12** [45], **13** and **14**

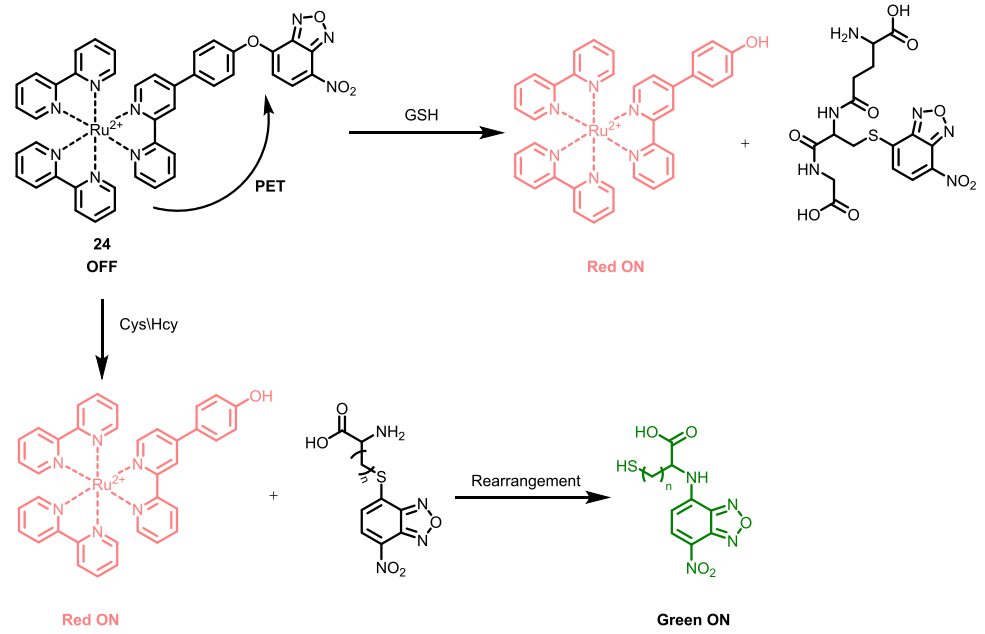

Fig. 9. The sensing mechanism of **24** to GSH and Cys/Hcy.

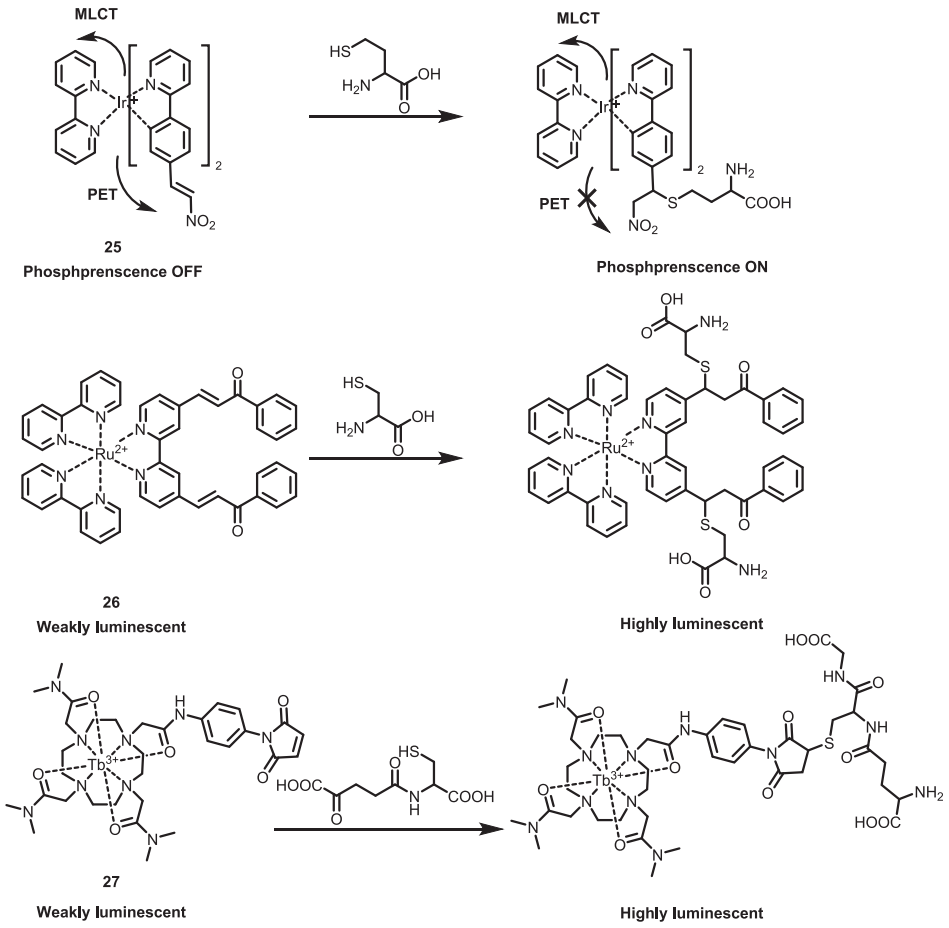

Fig. 10. The sensing mechanism of **25**–**27** for Cys/Hcy.

[46], in which two hydroxypyrenes were connected with a 2,2′-oxidiethanamino group, 1,2-ethanediamine and 2,2′-thiobis(ethylamine), respectively. As expected, the nearby Cu^{2+} quenched the fluorescence thoroughly after the formation of Cu^{2+} complexes. Similarly, the complexation of thiols can remove copper ions from the coordinating species and restore fluorescence. These probes can be used for the imaging of biothiols in living cells. Particularly, **13** can be used for tissue imaging with the help of two-photon microscopy.

16, **17** and **18** were constructed by introducing two chromophores into a probe through the coordination with ions [47–49]. **16** showed a good selectivity for GSH with a significant fluorescence enhancement, while **17** responded to all three biothiols (Fig. 7). **18** acted as a ratiometric fluorescent probe. The addition of biothiols induced a color change from blue to pink, while the emission peak at 585 nm was disappeared and the peak at 540 nm appeared.

The spectral properties and recognition of compounds **1**–**18** before and after biothiol identification were listed in Table 1, which can be used for comparison of biothiol identification performance of different probes.

3.2. Metal complex as a reporter

For this type of probes, the nucleophilicity and reducibility of sulfhydryl groups were used (Fig. 3b). Based on the reaction characteristics and strong electron absorption of 2,4-dinitrobenzene sulfonamide (DTNB/DNBS) or 2,4-dinitrophenylthio (DNS), Ji *et al.*, Tang *et al.*, Gao *et al.*, Zheng *et al.* Ye *et al.* reported **19**, **20**, **21**, **22** and **23** as probes for biothiols, respectively [50–54]. For those probes, electron's transfer from electron donor Ru or Ir to the intramolecular electron sink DTNB or DNBS resulting a non-luminescent state of those probes (**20** as an example, see Fig. 8). Once the sulfonamide or sulfonate ester cleaved by biothiols, phosphorescence at ~ 600 nm would be significantly enhanced. All the four probes can be used in biothiols imaging in live cells. For exam-

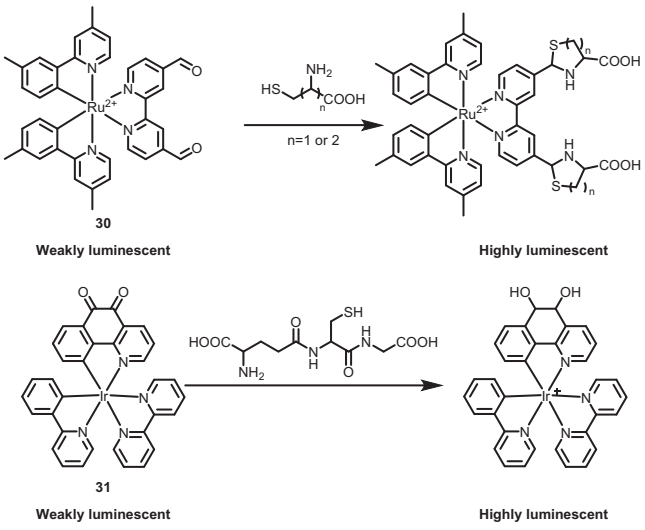

Fig. 11. The sensing mechanism of **30**–**31** for Cys/Hcy and GSH respectively.

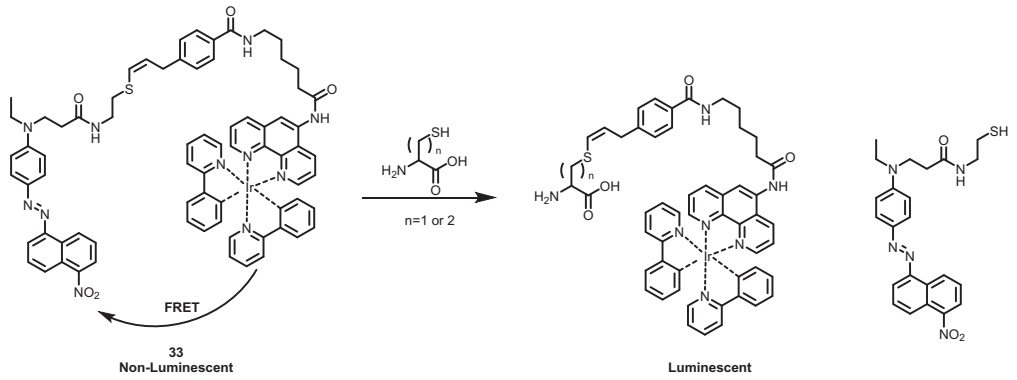

Fig. 12. The proposed mechanism of **33** for Cys/Hcy.

Table 2
Coordination Structure as Reporter.

Structure	λ_{abs} (nm)	λ_{em} (nm)	Biothiols	LOD	Responses	Ref.
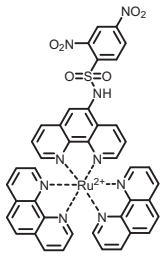 19	455	598	Cys	ND	A 90 fold enhancement was detected after adding Cys (ACN/Water, 1/4, v/v) and luminescence images of intracellular thiols was achieved.	[45]
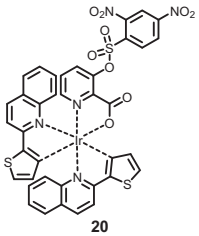 20	405	603	Cys Hcy	ND	Emission at 603 nm increased upon addition of Cys/Hcy (ACN/Water, pH 7.2, 4/1, v/v) and luminescent imaging of Cys/Hcy in live cells was obtained.	[46]
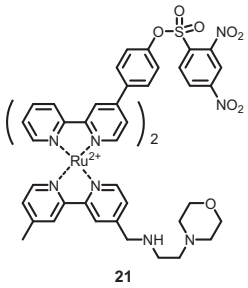 21	459	620	GSH Cys Hcy	62×10^{-9} M 146×10^{-9} M 145×10^{-9} M	Phosphorescence intensity at 620 nm increased after responding to biothiols (DMSO/HEPES, pH 7.0, 1/1, v/v) and images of biothiols in live cells and Daphnia magna were obtained.	[47]
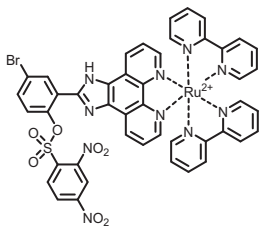 22	458	608	GSH Cys Hcy	0.27×10^{-6} M 0.47×10^{-6} M \	Large enhancement in emission intensity was detected after responding to biothiols (ACN/HEPES, pH 7.2, 1/100, v/v) with rapid response and live cell biothiol image was obtained.	[48]

(*continued on next page*)

Table 2 (*continued*)

Structure	λ_{abs} (nm)	λ_{em} (nm)	Biothiols	LOD	Responses	Ref.
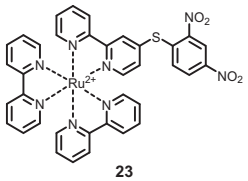 23	458	625	GSH Cys Hcy	1×10^{-6} M \ \	An 80 fold enhancement was detected after adding GSH (Ethanol/HEPES, pH 7.2, 1/4, v/v) and luminescence imaging of biothiols in living Daphnia magna was achieved.	[49]
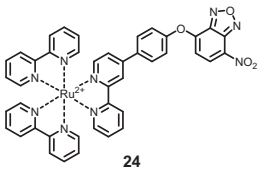 24	460 480	628 540	GSH Cys Hcy	83.32×10^{-9} M 86.54×10^{-9} M 85.36×10^{-9} M	GSH and Cys/Hcy was discriminated through steady-state luminescence analysis (Tris-HCl buffer pH 7.4) and visualization of biothiols in live cells, zebrafish, and mice was achieved.	[50]
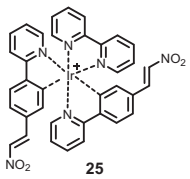 25	300–400	571	Hcy	47.6×10^{-9} M	Absorption peak decreased at 300–400 nm while emission peak increase at 571 nm with a rapid response to Hcy in 1 min and live cell image was also got.	[51]
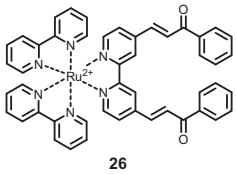 26	470	620	Cys	ND	A 30 fold luminescence enhancement at 620 nm was detected (HEPES) after responding to Cys and luminescence images of live cells and Zebrafish were obtained.	[52]
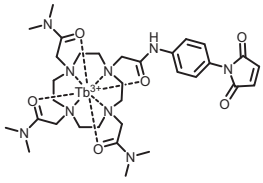 27	445	545	GSH	ND	The enzymatic reduction of GSSG to GSH in real time was observe (HEPES).	[53]
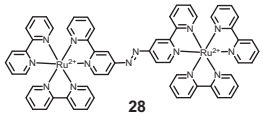 28	439	605	GSH Cys Hcy	2.42×10^{-7} M 2.29×10^{-7} M 2.27×10^{-7} M	A color change from gray to yellow of the solution was observed with a significant luminescence enhancement after responding to thiols (HEPES).	[54]
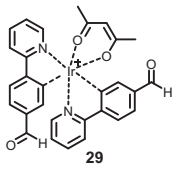 29	510	525	Hcy	ND	A color change from orange to yellow of the solution and a new emission bond at 520 nm was observed (DMSO/HEPES, 50 mM, pH 7.2, 9/1, v/v).	[55]
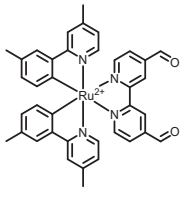 30	492	610	Cys Hcy	3×10^{-7} M 1×10^{-6} M	Enhancement in emission intensity was detected (ACN /HEPES, 50 mM, pH 7.2, 9/1, v/v).	[56]
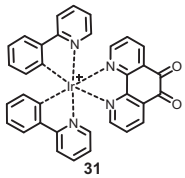 31	350	587	GSH	1.67×10^{-6} M	A luminescence enhancement at 587 nm was detected (ACN/HEPES, 10 mM, pH 7.0) with increasing the concentration of GSH.	[57]

Table 2 (*continued*)

Structure	λ_{abs} (nm)	λ_{em} (nm)	Biothiols	LOD	Responses	Ref.
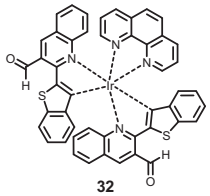 **32**	495	684	Cys Hcy	1.37×10^{-5} M 9.7×10^{-6} M	The absorption at 495 nm and the emission at 684 nm was increased upon addition the Cys or Hcy. Images of Cys/Hcy in live cells were obtained and could also monitor the Cys in living mice.	[58]
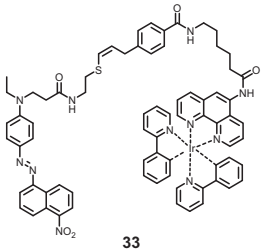 **33**	360	590	Cys Hcy	1.3×10^{-4} M (Hcy)	A luminescence enhancement at 590 nm was detected (ACN/PBS, pH 7.2) upon addition the Cys or Hcy.	[59]
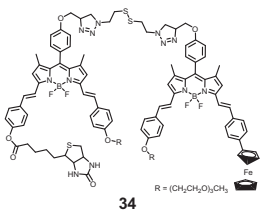 **34**	610	648	GSH	ND	A luminescence enhancement at 650 nm was detected (PBS, 0.5% Tween 80) upon addition of GSH. Images of GSH in live cells were obtained.	[60]
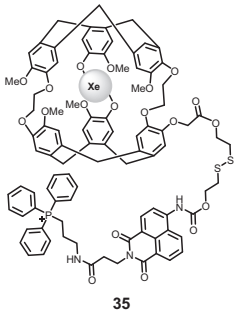 **35**	445	560	GSH Cys Hcy	ND	The color of solution changed from colorless to yellow and an enhancement of fluorescence intensity at 560 nm was detected (PBS, 20 mM, pH 7.4). The probe could target the mitochondria and detect the biothiol in cells.	[61]
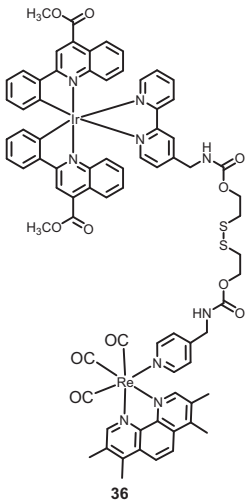 **36**	370	520	GSH	ND	The emission color change was observed from red to green (Methanol/PBS, pH 7.2, 7/3, v/v). The complexes targeted the mitochondria in living cells and could be used as thiol-responsive metallodrugs.	[62]

ple, **21** was used to observe biothiols in live Daphnia magna, proving its potential for in vivo imaging.

Liu *et al.* also took advantage of the strong electron withdrawing property of another group NBD [55] and constructed a complex probe **24** for biothiols detection and discrimination. Due to the photoinduced electron transfer (PET) from Ru(II) center to NBD, the probe was non-luminescent. The reaction with Cys/Hcy resulted in short-lived green-emitting NBD-NR and long-lived red-emitting Ru-OH, while the one with GSH produce Ru-OH and non-emissive NBD-SR. Time-gated luminescence (TGL) analysis can be used to detect total biothiols, while steady-state luminescence analysis allowed the discrimination of GSH and Cys/Hcy (Fig. 9). This probe was potential in biothiols detection and visualization in living system.

Probe **25**–**28** were also designed for biothiols sensing on the basis of PET mechanism, where the electron transfer took place from chromophore to the alkene moiety during photo excitation (Fig. 10). The Michael addition of biothiols to the electron deficient alkene group in **25**–**28** resulted in significant luminescent increases (Fig. 3b) [56–59].

Chen and coworkers reported the first luminescent Hcy selective sensor **29** [60]. Upon addition of Hcy, a blue shift in absorption spectra and an enhancement of the phosphorescence emission was detected, while no obvious changes were observed with the addition of Cys. The authors ascribed the emission quenching of the adduct **29**-Cys to the hypothesized inner electron transfer. Compounds **30**–**32** were designed as biothiols probes on the basis of the cyclic addition of biothiols to carbonyl groups (Fig. 3b). They all used obvious emission enhancement as a response signal to identify thiols [61–63] (Fig. 11). Among them, **32** had the potential to be used in *vivo* imaging.

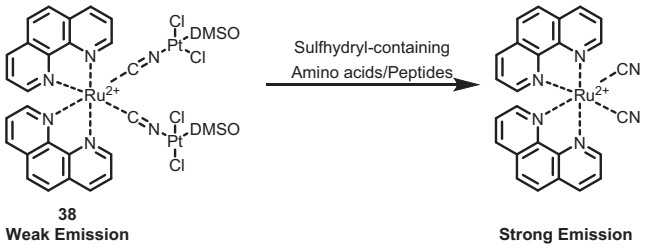

Fig. 13. The proposed mechanism of **38** for Biothiols and other amino.

33–**36** were typical FRET type fluorescent probes, where the donor and acceptor were connected by S-C or disulfide bonds (**33** as an example, see Fig. 12). When the S-C or disulfide bonds were reduced by sulfhydryl, the FRET donor and acceptor separated. The resulted emission changes acted as a response to the recognition of biothiols [64–67]. In probe **34** reported by Peng *et al.*, two different BODIPY were linked by a disulfide bond. One BODIPY acted as a donor, while the other one which was efficiently quenched by ferrocene acted as the receptor in FRET pairs. The sulfhydryl group of biothiols reduced the disulfide bond and broke donor-acceptor conjugate. The release donor BODIPY exhibited recovered emission. This probe had been used to image biothiols in living cells.

The spectral properties and recognition of compounds **19**–**36** before and after biothiol identification were listed in Table 2, which can be used for comparison of biothiol identification performance of different probes.

3.3. Metal complex as both receptor and reporter

37 reported by *Yang et al.* was a Cys and Hcy selective probe. It is characterized by the formation of metal complex at the presence

Table 3
Coordination Structure as both Receptor and Reporter.

Structure	λ_{abs} (nm)	λ_{em} (nm)	Biothiols	LOD/ Binding constant	Responses	Ref.
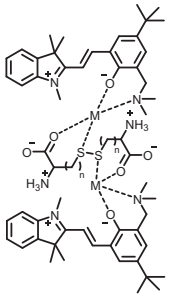 37	405	ND	Cys Hcy	ND	Absorbance at 532 nm greatly decreased, and the 378 nm absorption band moved to 405 nm concomitant with an increase in intensity after adding Cys or Hcy (Ethanol/ Water, pH 7.0).	[63]
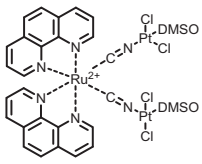 38	467	621	GSH Cys Hcy Met	$1.74 \pm 0.19 \times 10^5$ M^{-1} $8.40 \pm 0.23 \times 10^4$ M^{-1} $4.99 \pm 0.81 \times 10^4$ M^{-1} $2.92 \pm 0.25 \times 10^4$ M^{-1}	Emission of the complex moved from 595 to 621 nm and a significant enhancement in intensity was detected (DMF/H_2O, 1/1, v/v).	[64]
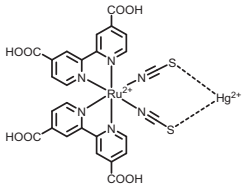 39	508	ND	GSH Cys	$52 \pm 2 \times 10^{-9}$ M (GSH) $57 \pm 3 \times 10^{-9}$ M (Cys)	Absorbance at 461 nm decreased and absorbance at 508 nm increased after addition of Cys and GSH (Methanol/ HEPES, 10 mM, pH 7.4, 1/1, v/v).	[65]
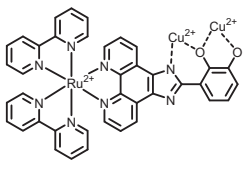 40	465	585	GSH Cys Hcy	1.1×10^{-6} M (GSH)	Phosphorescence turned on in the presence of biothiols (HEPES) and successfully applied for probing endogenous thiols in the living cells.	[66]

of the probe, biothiols and metal ion at the same time [68]. This probe used a spiropyran derivative as the chromophore. In the 10% aqueous ethanol at pH 7.0, the spiropyran derivative had a main absorption peak at 532 nm. When the metal ion (Cu^{2+} or Hg^{2+}) and Cys were added to the solution at the same time, the absorption at 523 nm significantly decreased and the 378 nm absorption increased obviously. A change in color from red-viole to yellow was visible to the naked eye.

38–**40** were constructed based on the strong coordination capacity of sulfur [69–71]. In **38**, due to the cyano coordination to the electron-accepting $Pt(DMSO)Cl_2$ moieties, ^{3}MLCT emission of *cis*-$[Ru(phen)_2(CN)_2]$ was quenched. When the Pt(II) Coordination was displaced by GSH, Cys or Hcy, the cyano bridge cleavaged and the orange-red ^{3}MLCT luminescence recovered (Fig. 13). A similar displacement strategy was also used in **39** and **40**.

The spectral properties and recognition of compounds **37**–**40** before and after biothiol identification were listed in Table 3, which can be used for comparison of biothiol identification performance of different probes.

4. Metal complex as an imaging tool

The distribution of biothiols in cells is dynamic and heterogeneous. Fluorescence imaging can indicate the location and distribution of biothiols in cells, and even the local concentrations. Among them, the homeostasis of biothiols is closely related to a variety of physiological processes, which requires fluorescent probes to achieve reversible binding to biothiols, so as to realize real-time monitoring of the dynamic concentration changes of thiols. As a reversible binding force, coordination is expected to play an important role in selective recognition.

To date, a large number of metal complexes have been reported for living cell imaging of biothiols. As we discussed before, probes for biothiols based on metal complex are divided into three categories: metal complex as a receptor [39–44,46], metal complex as a reporter, and metal complex as both receptor and reporter [50,51,53,56,65–67,71]. All these three type fluorescent probes had the potentials to image biothiols in living cells. Fig. 14 showed the application of probe **20** in cell imaging. For tissue imaging, Hu *et al.* designed a copper complex of the pyrene derivative **11**. After identified GSH, two-photon imaging of hippocampus tissue sections was realized by using the multi-photon absorption properties of fluorophore pyrene (Fig. 15) [45].

Furthermore, Wu *et al.* developed probe **32** based on the iridium (III) complex with NIR-emission which was realized in *vivo* imaging of Cys in mice (Fig. 16) [63]. In addition, transition metal complexes **21**, **23**, **24**, **26** displayed unique optical properties, including long wavelength absorption, phosphorescent emission, large stokes shift. They probes had been successfully used in imaging of biothiols in zebrafish [55,57], daphnia [52,54] and live mice[55].

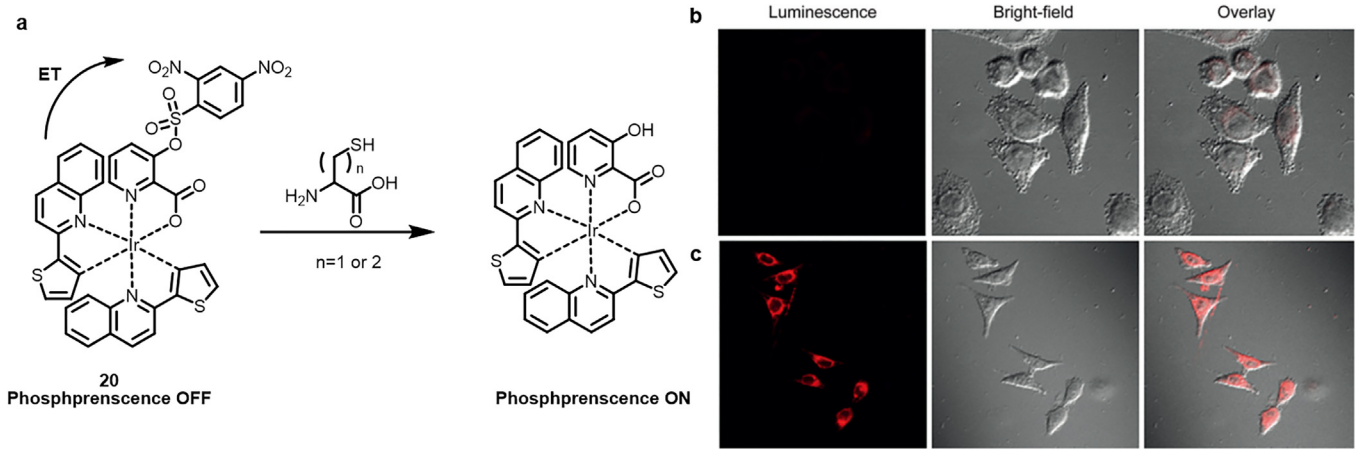

Fig. 14. The application of **20** in biothiols imaging in living cells. a) Sensing mechanism of "OFF-ON" phosphorescen **20**. Luminescence images of **20** in Hela cells, b) Hela cells incubated with N-ethylmaleimide before incubated with **20**, c) Hela cells incubated with **20**. Wherein, Fig. 14b and c is reprinted from Ref. [51] with permission from Copyright 2013, Wiley-VCH.

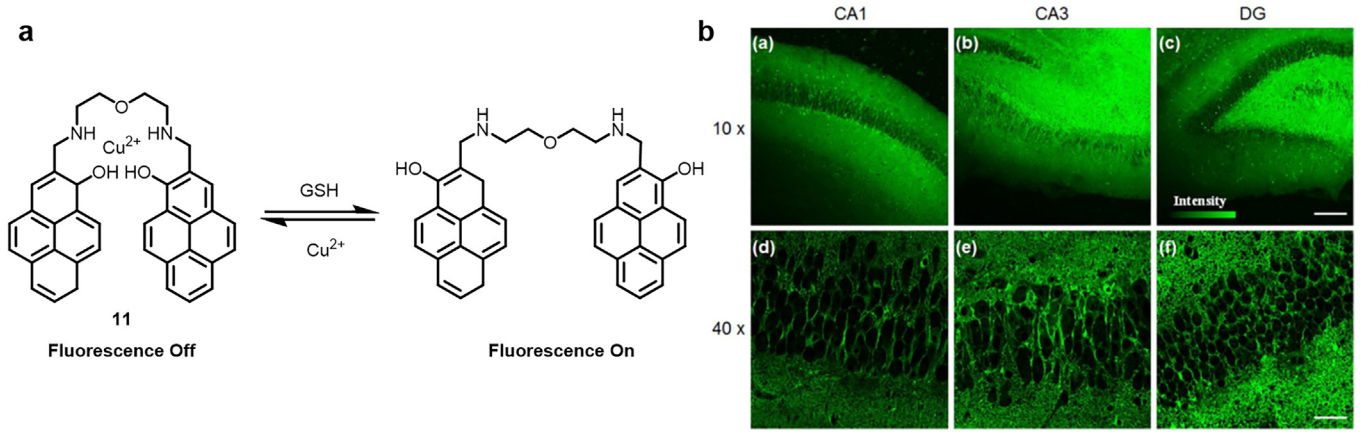

Fig. 15. The application of metal complex **11** in biothiols imaging in hippocampus tissue sections. a) "Off-On" response of **11**. b) Two-photon microscopy imaging of the CA1, CA3, and DG regions stained with **11**, respectively. Wherein, Fig. 15b is reprinted from Ref. [45] with permission from Copyright 2015, American Chemical Society.

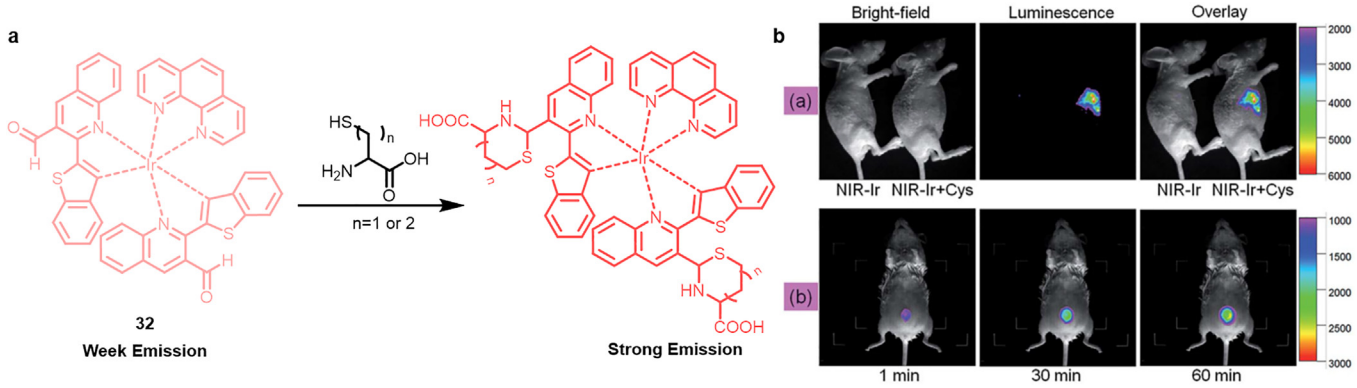

Fig. 16. The application of **32** in biothiols imaging in live mice. a) Sensing mechanism of probes 32. b) Top row: In vivo NIR images of **32**, the mice in the left was pretreated by normal saline and the other one was injected with Cys. Bottom row: live mice images of **32** respond to Cys over time. Wherein, Fig. 16b is reprinted from Ref. [63] with permission from Copyright 2017, The Royal Society of Chemistry.

5. Concluding remarks

Many significant advances have been made in the research of biothiol fluorescent probes, including the development of the early design principles of biothiol sensing, the later realization of selective recognition of different biothiols, and the reversible covalent linkage and dissociation of sulfhydryl groups [8,72–74]. From the perspective of the binding force of recognition, fluorescent probes mainly refer to the nucleophilic reactivity and coordination ability of sulfhydryl groups, while many researches have focused on the nucleophilic properties of sulfhydryl groups. This article systematically reviews metal complexes as receptors or reporters to develop biothiol fluorescent probes, and introduces the performance of these probes in detail. It is believed that future research will pay more attention to coordination in the probe design.

In the currently reported biothiol fluorescent probes, the core of recognition is focused on the nucleophilic reaction ability of sulfhydryl S, which will inevitably cause the probes that have been reported to recognize thiol in the cell to face competition with other sulfhydryl groups in the organism. The detection and imaging of biothiols in biological samples requires the real selective recognition of biothiols, rather than the recognition of sulfhydryl groups. This has become the focus of current research. The solution includes the overall consideration of the three functional units of biothiols R, S, and H, and the introduction and synergistic use of various chemical forces. As a reversible binding force, coordination is expected to play an important role in selective recognition.

Declaration of Competing Interest

The authors declare that they have no known competing financial interests or personal relationships that could have appeared to influence the work reported in this paper.

Acknowledgements

This work is supported by the National Natural Science Foundation of China (21878286), Dalian Institute of Chemical Physics (DMTO201603, TMSR201601).

References

[1] A. Meister, M.E. Anderson, 52 (1983) 711-760.
[2] G. Hu, H. Jia, L. Zhao, D.-H. Cho, J. Fang, Chin. Chem. Lett. 30 (2019) 1704–1716.
[3] R. Franco, O.J. Schoneveld, A. Pappa, M.I. Panayiotidis, Arch. Physiol. Biochem. 113 (2007) 234–258.
[4] D.M. Townsend, K.D. Tew, H. Tapiero, Biomed. Pharmacother. 57 (2003) 145–155.
[5] S. Zhang, C.N. Ong, H.M. Shen, Cancer Lett 208 (2004) 143–153.
[6] G.K. Balendiran, R. Dabur, D. Fraser, Cell Biochem. Funct. 22 (2004) 343–352.
[7] G.Y. Wu, Y.Z. Fang, S. Yang, J.R. Lupton, N.D. Turner, J. Nutr. 134 (2004) 489–492.
[8] K. Umezawa, M. Yoshida, M. Kamiya, T. Yamasoba, Y. Urano, Nature Chem. 9 (2017) 279–286.
[9] J. Yin, Y. Kwon, D. Kim, D. Lee, G. Kim, Y. Hu, J.H. Ryu, J. Yoon, Nat. Protoc. 10 (2015) 1742–1754.
[10] S. Shahrokhian, Anal. Chem. 73 (2001) 5972–5978.
[11] J. Yin, W. Ren, G. Yang, J. Duan, X. Huang, R. Fang, C. Li, T. Li, Y. Yin, Y. Hou, S.W. Kim, G. Wu, Mol Nutr Food Res 60 (2016) 134–146.
[12] H.S. Jung, X. Chen, J.S. Kim, J. Yoon, Chem. Soc. Rev. 42 (2013) 6019–6031.
[13] H. Chen, Y. Tang, W. Lin, TrAC, Trends Anal. Chem. 76 (2016) 166–181.
[14] L. Yu, Y. Qiao, L. Miao, Y. He, Y. Zhou, Chin. Chem. Lett. 29 (2018) 1545–1559.
[15] J. Xu, H. Yuan, L. Zeng, G. Bao, Chin. Chem. Lett. 29 (2018) 1456–1464.
[16] M. Li, P. Cui, K. Li, J. Feng, M. Zou, X. Yu, Chin. Chem. Lett. 29 (2018) 992–994.
[17] L. Zhou, L. Xie, C. Liu, Y. Xiao, Chin. Chem. Lett. 30 (2019) 1799–1808.
[18] J. Zhu, P. Jia, N. Li, S. Tan, J. Huang, L. Xu, Chin. Chem. Lett. 29 (2018) 1445–1450.
[19] Y.-F. Kang, L.-Y. Niu, Q.-Z. Yang, Chin. Chem. Lett. 30 (2019) 1791–1798.
[20] J. Wang, H.-B. Liu, Z. Tong, C.-S. Ha, Coord. Chem. Rev. 303 (2015) 139–184.
[21] R. Zhang, J. Yong, J. Yuan, Z. Ping Xu, Coord. Chem. Rev., 408 (2020).
[22] S. Lee, J. Li, X. Zhou, J. Yin, J. Yoon, Coord. Chem. Rev. 366 (2018) 29–68.
[23] J. Dai, C. Ma, P. Zhang, Y. Fu, B. Shen, Dyes Pigm. 177 (2020).
[24] K. Wang, H. Peng, B. Wang, J. Cell. Biochem. 115 (2014) 1007–1022.
[25] X. Chen, Y. Zhou, X. Peng, J. Yoon, Chem. Soc. Rev. 39 (2010) 2120–2135.
[26] C. Yin, F. Huo, J. Zhang, R. Martinez-Manez, Y. Yang, H. Lv, S. Li, Chem. Soc. Rev. 42 (2013) 6032–6059.
[27] L.Y. Niu, Y.Z. Chen, H.R. Zheng, L.Z. Wu, C.H. Tung, Q.Z. Yang, Chem. Soc. Rev. 44 (2015) 6143–6160.
[28] C.X. Yin, K.M. Xiong, F.J. Huo, J.C. Salamanca, R.M. Strongin, Angew. Chem. Int. Ed. 56 (2017) 13188–13198.
[29] A.P. de Silva, H.Q.N. Gunaratne, T. Gunnlaugsson, A.J.M. Huxley, C.P. McCoy, J.T. Rademacher, T.E. Rice, Chem. Rev. 97 (1997) 1515–1566.
[30] G. Qu, Y. Zhang, X. Ma, Chin. Chem. Lett. 30 (2019) 1809–1814.
[31] Z. Liu, W. He, Z. Guo, Chem. Soc. Rev. 42 (2013) 1568–1600.
[32] R. Peng, Y. Xu, Q. Cao, Chin. Chem. Lett. 29 (2018) 1465–1474.
[33] M.S. Han, D.H. Kim, Tetrahedron 60 (2004) 11251–11257.
[34] Y. Fu, H. Li, W. Hu, D. Zhu, Chem Commun (Camb) (2005) 3189–3191.
[35] X.F. Yang, P. Liu, L. Wang, M. Zhao, J Fluoresc 18 (2008) 453–459.
[36] Y.K. Yang, S. Shim, J. Tae, Chem Commun (Camb) 46 (2010) 7766–7768.
[37] O.G. Tsay, K.M. Lee, D.G. Churchill, New J. Chem. 36 (2012).
[38] R. Peng, L. Lin, X. Wu, X. Liu, X. Feng, J. Org. Chem. 78 (2013) 11602–11605.
[39] H.S. Jung, J.H. Han, Y. Habata, C. Kang, J.S. Kim, Chem Commun (Camb) 47 (2011) 5142–5144.
[40] X. Yu, K. Wang, D. Cao, Z. Liu, R. Guan, Q. Wu, Y. Xu, Y. Sun, X. Zhao, Sens. Actuators B Chem. 250 (2017) 132–138.
[41] Y. Yang, X. Yang, K. Zhou, M. Jin, W. Li, J. Photochem. Photobiol. A 383 (2019).
[42] H. Jia, M. Yang, Q. Meng, G. He, Y. Wang, Z. Hu, R. Zhang, Z. Zhang, Sensors 16 (2016).
[43] Z.-Q. Hu, L.-L. Sun, Y.-Y. Gu, Y. Jiang, Sens. Actuators B Chem. 212 (2015) 220–224.
[44] G. He, J. Li, Z. Wang, C. Liu, X. Liu, L. Ji, C. Xie, Q. Wang, Tetrahedron 73 (2017) 272–277.
[45] Y. Hu, C.H. Heo, G. Kim, E.J. Jun, J. Yin, H.M. Kim, J. Yoon, Anal. Chem. 87 (2015) 3308–3313.
[46] N. Kwon, J. Hong, G. Kim, E.J. Jun, J. Yoon, Dyes Pigm. 173 (2020).
[47] W. Chen, X. Wu, L. Pu, Tetrahedron Lett. 58 (2017) 1781–1783.
[48] R. Singh, G. Das, Analyst 144 (2019) 567–572.
[49] M.D. Gholami, S. Manzhos, P. Sonar, G.A. Ayoko, E.L. Izake, Analyst 144 (2019) 4908–4916.

[50] S.M. Ji, H.M. Guo, X.L. Yuan, X.H. Li, H.D. Ding, P. Gao, C.X. Zhao, W.T. Wu, W.H. Wu, J.Z. Zhao, Org. Lett. 12 (2010) 2876–2879.
[51] Y. Tang, H.R. Yang, H.B. Sun, S.J. Liu, J.X. Wang, Q. Zhao, X.M. Liu, W.J. Xu, S.B. Li, W. Huang, Chemistry 19 (2013) 1311–1319.
[52] Q. Gao, W. Zhang, B. Song, R. Zhang, W. Guo, J. Yuan, Anal. Chem. 89 (2017) 4517–4524.
[53] Z.-B. Zheng, J.-C. Cui, Y.-F. Han, Y.-Q. Ge, J. Zuo, W.-X. Hao, Anal. Methods 11 (2019) 2341–2350.
[54] Z. Ye, Q. Gao, X. An, B. Song, J. Yuan, Dalton. Trans. 44 (2015) 8278–8283.
[55] C. Liu, J. Liu, W. Zhang, Y.L. Wang, Q. Liu, B. Song, J. Yuan, R. Zhang, Advanced Science, (2020).
[56] M. Zhao, Y. Pan, X. Wang, X.-W. Gao, D. Chao, New J. Chem. 42 (2018) 5508–5513.
[57] Y. Li, N. Shi, M. Li, New J. Chem. 43 (2019) 18517–18524.
[58] B.K. McMahon, T. Gunnlaugsson, J. Am. Chem. Soc. 134 (2012) 10725–10728.
[59] G.Y. Li, J.P. Liu, H.Y. Huang, Y. Wen, H. Chao, L.N. Ji, J. Inorg. Biochem. 121 (2013) 108–113.
[60] H.L. Chen, Q. Zhao, Y.B. Wu, F.Y. Li, H. Yang, T. Yi, C.H. Huang, Inorg. Chem. 46 (2007) 11075–11081.
[61] M.J. Li, C.Q. Zhan, M.J. Nie, G.N. Chen, X. Chen, J. Inorg. Biochem. 105 (2011) 420–425.
[62] Z. Mao, J. Liu, T.S. Kang, W. Wang, Q.B. Han, C.M. Wang, C.H. Leung, D.L. Ma, Sci. Technol. Adv. Mater. 17 (2016) 109–114.
[63] Y. Wu, R. Wu, H. Li, H. Zeng, Y. Li, Q. Wang, M. Shi, X. Fan, RSC Adv. 7 (2017) 52621–52625.
[64] H.Y. Shiu, M.K. Wong, C.M. Che, Chem. Commun. (Camb) 47 (2011) 4367–4369.
[65] W.J. Shi, P.C. Lo, S. Zhao, R.C. Wong, Q. Wang, W.P. Fong, D.K. Ng, Dalton. Trans. 45 (2016) 17798–17806.
[66] Q. Zeng, Q. Guo, Y. Yuan, Y. Yang, B. Zhang, L. Ren, X. Zhang, Q. Luo, M. Liu, L.S. Bouchard, X. Zhou, Anal. Chem. 89 (2017) 2288–2295.
[67] S.P. Li, J. Shum, K.K. Lo, Dalton. Trans. 48 (2019) 9692–9702.
[68] N. Shao, J.Y. Jin, S.M. Cheung, R.H. Yang, W.H. Chan, T. Mo, Angew. Chem. Int. Ed. 45 (2006) 4944–4948.
[69] C.F. Chow, B.K.W. Chiu, M.H.W. Lam, W.Y. Wong, J. Am. Chem. Soc. 125 (2003) 7802–7803.
[70] Y. Hao, D. Xiong, L. Wang, W. Chen, B. Zhou, Y.-N. Liu, Talanta 115 (2013) 253–257.
[71] P. Zhang, Y. Wang, W. Huang, Z. Zhao, H. Li, H. Wang, C. He, J. Liu, Q. Zhang, Sens. Actuators B Chem. 255 (2018) 283–289.
[72] Z. Liu, X. Zhou, Y. Miao, Y. Hu, N. Kwon, X. Wu, J. Yoon, Angew. Chem. Int. Ed. 56 (2017) 5812–5816.
[73] X. Jiang, J. Chen, A. Bajić, C. Zhang, X. Song, S.L. Carroll, Z.-L. Cai, M. Tang, M. Xue, N. Cheng, C.P. Schaaf, F. Li, K.R. MacKenzie, A.C.M. Ferreon, F. Xia, M.C. Wang, M. Maletić-Savatić, J. Wang, Nat. Commun. 8 (2017) 16087.
[74] Z. Chang, F. Liu, L. Wang, M. Deng, C. Zhou, Q. Sun, J. Chu, Chin. Chem. Lett. 30 (2019) 1856–1882.